*Journal of American Chemical Society*

**Supplementary Information**

# A synthetic replicator drives a propagating reaction-diffusion front

Ilaria Bottero, Jürgen Huck, Tamara Kosikova and Douglas Philp*

School of Chemistry and EaStCHEM, University of St Andrews,
North Haugh, St Andrews, Fife KY16 9ST, United Kingdom

*Corresponding author: d.philp@st-andrews.ac.uk

**Table of contents:**

## 1. General experimental procedures

Chemicals were purchased from ABCR GmbH & Co, Alfa Aeasar, Apollo Scientific Ltd., Fisher Scientific UK Ltd., TCI UK Ltd., Sigma Aldrich Company Ltd. or VWR International Ltd. Where appropriate, all non-aqueous reactions were carried out under inert atmosphere. Brine refers to a saturated solution of sodium chloride. Dry THF, PhMe and $CH_2Cl_2$ were obtained using and MBraun MS SPS-800 solvent purification system, where solvents are dried by passage through filter columns and dispensed under argon atmosphere. Thin layer chromatography (TLC) analysis was performed using MACHEREY-NAGEL GmbH & Co. POLYGRAM SIL G/UV254 plates. Once developed, plates were air-dried and visualised under a UV lamp (λmax 254 or 366 nm).

Melting points were determined using an Electrothermal 9200 melting point apparatus and are uncorrected. Mass spectra were recorded on a Micromass GCT spectometer for electron impact ionisation (EI) operating at 70 eV or chemical ionisation (CI) using isobutane as the ionising gas. Electrospray ionisation spectra (ESI) were performed on a Micromass LCT spectrometer operating in positive or negative mode from solutions of methanol, acetonitrile or water. *m*/*z* values are reported in Daltons and followed by their percentage abundance in parentheses.

$^1$H NMR spectra were recorded on a Bruker Avance 500 (500.1 MHz), a Varian UNITYplus 500 (500.1 MHz), a Bruker Avance II 400 (400.1 MHz) or a Bruker Avance 300 (300.1 MHz) spectrometer using the deuterated solvent as the lock and the residual solvent as the internal reference in all cases ($\delta_H$ $CHCl_3$ = 7.26 ppm, $\delta_H$ DMSO = 2.50 ppm). $^{13}$C NMR spectra were recorded on a Bruker Avance III 500 (125.8 MHz), Bruker Avance II 400 (100.6 MHz) or a Bruker Avance 300 (75.5 MHz) spectrometer using the CPD or DEPTQ pulse sequences with broadband proton decoupling using the deuterated solvent as the lock and the residual solvent as the internal reference in all cases ($\delta_C$ $CHCl_3$ = 77.16 ppm, $\delta_C$ DMSO = 39.52 ppm). The chemical shift information ($\delta_c$) for each resonance signal are given in units of parts per million (ppm) relative to trimethylsilane (TMS) where $\delta_c$ TMS = 0.00 ppm. All $^1$H and $^{13}$C spectra were analysed using iNMR software (Version 5.4.7, Mestrelab Research, 2015).

## 2. Synthetic procedures and spectroscopic data

Synthesis of the maleimide **2**[1] has been reported previously. $^{1}H$ and $^{13}C$ spectra for each compound are provided at the end of the supplementary information.

### (Anthracen-9-ylethynyl)trimethylsilane[2,3]

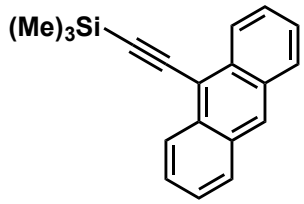


A solution of 9-bromoanthracene (4.00 g, 15.6 mmol), CuI (223 mg, 1.17 mmol), $PdCl_2(PPh_3)_2$ (543 mg, 774 μmol) and $PPh_3$ (408 mg, 1.55 mmol) in dry $Et_3N$ (200 mL) was reacted with ethynyltrimethylsilane (3.82 g, 39.1 mmol) under argon atmosphere at 80 ˚C for 24 hours. The solution obtained was filtered through celite and concentrated under reduced pressure. The crude product was purified by silica gel flash column chromatography (hexane) affording the product as a yellow solid (3.51 g, 82%).

**M.p.:** 80.3-83.5 ˚C. **$^{1}H$ NMR** (300.1 MHz, $CDCl_3$): $\delta_H$ 8.57 (dd, *J* = 8.7, 1.1 Hz, 2H), 8.42 (s, 1H), 8.00 (dt, *J* = 8.4, 0.6 Hz, 2H), 7.59 (ddd, *J* = 8.6, 6.6, 1.4 Hz, 2H), 7.50 (ddd, *J* = 8.2, 6.7, 1.4 Hz, 2H), 0.44 (s, 9H). **$^{13}C$ NMR** (75.5 MHz, $CDCl_3$): $\delta_C$ 133.0 (Ar*C*, 2C), 131.2 (Ar*C*, 2C), 128.8 (Ar*C*H, 2C), 128.0 (Ar*C*H), 126.9 (Ar*C*H, 2C), 126.8 (Ar*C*H, 2C), 125.8 (Ar*C*H, 2C), 117.2 (Ar*C*), 106.3 (*C*≡C), 101.7 (*C*≡C), 0.4 (*C*H$_3$). **MS** (CI+) *m/z* 274 (100%, $[M]^+$), 275 (85%, $[M+H]^+$). **HRMS** (*m/z*) $[M+H]^+$ calculated for $C_{19}H_{19}Si$ 275.1251, found 275.1249.

### 9-((4-nitrophenyl)ethynyl)anthracene[4]

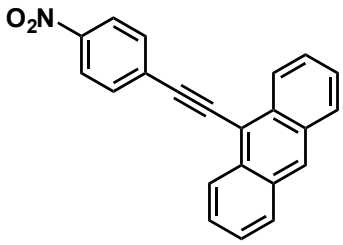


The protected acetylene (3.20 g, 11.7 mmol) was dissolved in a 1:1 mixture of dry THF and MeOH (80 mL). $K_2CO_3$ (8.08 g, 58.5 mmol) was added and the mixture was stirred under argon atmosphere for four hours at room temperature, before being quenched with

water (80 mL). The aqueous phase was extracted with $CH_2Cl_2$ (3 × 120 mL). The organic fractions were collected, dried over $MgSO_4$, filtered and concentrated to 10% of the original volume. $Et_3N$ (100 mL) was added and the solution was reduced to 10% of its original volume. This step was repeated twice, before $Et_3N$ (250 mL) was added as solvent for the following conversion. CuI (154 mg, 811 μmol), $PdCl_2(PPh_3)_2$ (372 mg, 530 μmol), $PPh_3$ (277 mg, 1.06 mmol) and 1-iodo-4-nitrobenzene (2.65 g, 10.6 mmol) were added to the solution, which was stirred at 50 ˚C for 24 hours under argon atmosphere. The solution was filtered through celite, concentrated *in vacuo* and purified by silica gel flash column chromatography (hexane:EtOAc, 10:1) to afford the product as a red solid (2.91 g, 85%).

**M.p.**: 203.2-205.6 ˚C. **$^1$H NMR** (500.1 MHz, $CDCl_3$): $\delta_H$ 8.59 (dq, J = 8.7, 0.9 Hz, 2H), 8.51 (s, 1H), 8.30-8.28 (m, 2H), 8.06-8.04 (m, *J* = 0.6 Hz, 2H), 7.89-7.86 (m, 2H), 7.64 (ddd, *J* = 8.7, 6.6, 1.3 Hz, 2H), 7.55 (ddd, *J* = 8.2, 6.7, 1.3 Hz, 2H). **$^{13}$C NMR** (125.8 MHz, $CDCl_3$): $\delta_C$ 147.1 (*C*$NO_2$), 133.0 (Ar*C*, 2C), 132.3 (Ar*C*H, 2C), 131.2 (Ar*C*, 2C), 130.6 (Ar*C*), 129.3 (Ar*C*H), 129.1 (Ar*C*H, 2C), 127.3 (Ar*C*H, 2C), 126.5(Ar*C*H, 2C), 126.0 (Ar*C*H, 2C), 124.0 (Ar*C*H, 2C), 115.9 (Ar*C*), 98.9 (*C*≡C), 92.0 (*C*≡C). **MS** (CI+) *m/z* 324 (100%, $[M+H]^+$). **HRMS** (*m/z*) $[M+H]^+$ calculated for $C_{22}H_{14}NO_2$ 324.1019, found 324.1031.

***N*-(4-(anthracen-9-ylethynyl)phenyl)hydroxylamine**

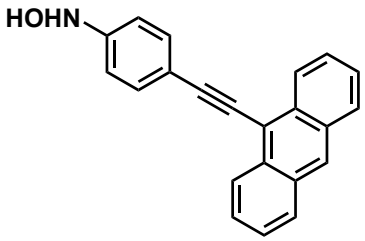


A solution of 9-((4-nitrophenyl)ethynyl)anthracene (100 mg, 0.309 mmol) in THF (10 mL) was mixed with rhodium (5 wt. % on carbon, 40.0 mg), before hydrazine monohydrate (92.9 mg, 90.0 μL, 1.86 mmol) was added dropwise. The reaction was stirred for 20 minutes at which point TLC analysis (chex:EtOAc, 3:1, staining with ninhydrin) showed complete conversion to product. The reaction mixture was filtered through celite and washed with further portion of THF. The organic solution was concentrated *in vacuo* (at 25 °C), re-dissolved in $CH_2Cl_2$ (5 mL) and precipitated with petroleum ether 40 – 60 °C. The resulting precipitate was filtered under suction, affording the target product as an orange powder, sufficiently pure for further

reaction (78.1 mg, 81%).

**$^1$H NMR** (400.3 MHz, $CDCl_3$): $\delta_H$ 8.67-8.64 (m, 2H), 8.42 (s, 1H), 8.03-8.01 (m, 2H), 7.72-7.68 (m, 2H), 7.61-7.49 (m, 4H), 7.08-7.05 (m, 2H), 6.91 (br s, 1H), 5.22 (br s, 1H). **MS** (ES–) *m/z* 308 (100%, $[M–H]^-$).

**(*Z*)-4-(anthracen-9-ylethynyl)-*N*-(4-((6-methylpyridin-2-yl)carbamoyl)benzylidene) aniline oxide Nitrone 1b**

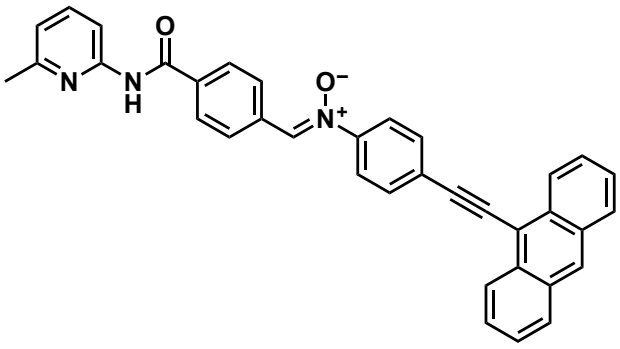


*N*-(4-(anthracen-9-ylethynyl)phenyl)hydroxylamine (490 mg, 1.60 mmol) was dissolved in $CHCl_3$ (3 mL) and added to a solution of 4-formyl-*N*-(6-methylpyridin-2-yl)benzamide (384 mg, 1.60 mmol) in ethanol (10 mL). The reaction mixture was kept for two days at –17 ˚C. The formed precipitate was filtered, washed with hexane and dried under vacuum (450 mg, 53%).

**M.p.**: 203.0 ˚C (decomp.). **$^1$H NMR** (500.1 MHz, $CDCl_3$): $\delta_H$ 8.65-8.63 (m, 2H), 8.57-8.54 (m, 3H), 8.49 (s, 1H), 8.20 (d, *J* = 8.2 Hz, 1H), 8.10 (s, 1H), 8.07-8.04 (m, 4H), 7.93-7.89 (m, 4H), 7.69-7.62 (m, 3H), 7.56-7.53 (m, *J* = 1.3 Hz, 2H), 6.97 (d, *J* = 7.5 Hz, 1H), 2.50 (s, 3H). **$^{13}$C NMR** (125.8 MHz, $CDCl_3$): $\delta_C$ 164.7 (*C*O), 157.2 (Py*C*), 150.7 (Py*C*), 148.3 (Ar*C*), 139.0 (Py*C*H), 135.9 (Ar*C*), 133.9 (Ar*C*), 133.5 (*C*H-NO), 132.9 (Ar*C,* 2C), 132.6 (Ar*C*H, 2C), 131.3 (Ar*C,* 2C), 129.3 (Ar*C*H, 2C), 129.0 (Ar*C*H, 2C), 128.6 (Ar*C*H), 127.7 (Ar*C*H, 2C), 127.1 (Ar*C*H, 2C), 126.7 (Ar*C*H, 2C), 126.2 (Ar*C*), 126.0 (Ar*C*H, 2C), 122.1 (Ar*C*H, 2C), 119.8 (Py*C*H), 116.5 (Ar*C*), 111.1 (Py*C*H), 99.3 (*C*≡C), 89.2 (*C*≡C), 24.2 (*C*H$_3$). **MS** (ES+) *m/z* 532 (100%, $[M+H]^+$), 554 (20%). **HRMS** (ES+) (*m/z*) $[M+H]^+$ calculated for $C_{36}H_{26}N_3O_2$ 532.2025, found 532.2018.

**2-(4-(2-(4-(anthracen-9-ylethynyl)phenyl)-3-(4-((6-methylpyridin-2-yl)carbamoyl)phenyl)-4,6-dioxotetrahydro-2H-pyrrolo[3,4-d]isoxazol-5(3H)-yl)phenyl)acetic acid Template *trans*-3b**

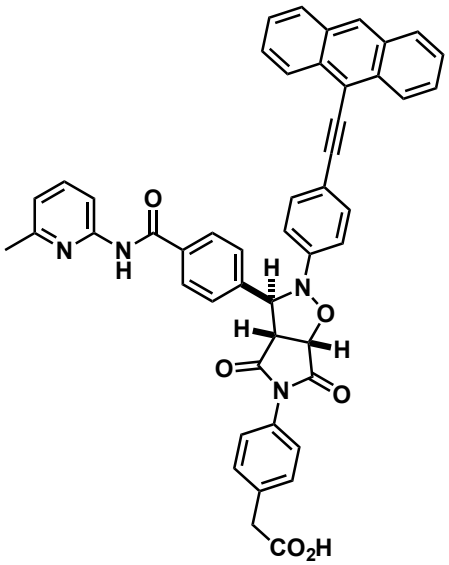


(*Z*)-4-(anthracen-9-ylethynyl)-*N*-(4-((6-methylpyridin-2-yl)carbamoyl)benzylidene) aniline oxide **1b** (26.6 mg, 50.2 μmol) was dissolved in $CHCl_3$ (5 mL) and reacted with maleimide **2** (11.6 mg, 50.0 μmol) for 24 hours. The solution was concentrated and the crude product was further purified by recrystallisation (THF:hexane, 100:1) in essentially quantitative yield.

**M.p.**: 232.8 ˚C (decomp.). **$^1$H NMR** (400.1 MHz, $d_6$-DMSO): $\delta_H$ 10.84 (s, 1H), 8.68 (s, 1H), 8.59 (d, *J* = 8.7 Hz, 2H), 8.17 (d, *J* = 8.5 Hz, 2H), 8.11 (d, *J* = 8.3 Hz, 2H), 8.03 (d, *J* = 8.2 Hz, 1H), 7.85-7.66 (m, 7H), 7.61 (t, *J* = 7.4 Hz, 2H), 7.39 (d, *J* = 8.7 Hz, 2H), 7.29 (d, *J* = 8.3 Hz, 2H), 7.06 (d, *J* = 7.5 Hz, 1H), 6.73 (d, *J* = 8.3 Hz, 2H), 6.14 (s, 1H), 5.54 (d, *J* = 7.3 Hz, 1H), 4.24 (d, *J* = 7.4 Hz, 1H), 3.55 (s, 2H), 2.47 (s, 3H). **$^{13}$C NMR** (100.6 MHz, $d_6$-DMSO): $\delta_C$ 174.2 (*C*=O), 173.1 (*C*=O), 172.3 (*C*OOH), 165.5 (*C*=O), 156.2 (Py*C*), 151.2 (Py*C*), 149.0 (Ar*C*), 142.5 (Ar*C*), 138.9 (Ar*C*H), 135.9 (Ar*C*), 133.5 (Ar*C*), 132.6 (Ar*C*H, 2C), 131.7 (Ar*C*, 2C), 130.8 (Ar*C*, 2C), 130.0 (Ar*C*H, 2C), 130.0 (Ar*C*), 128.9 (Ar*C*H, 2C), 128.4 (Ar*C*H, 2C), 127.8 (Ar*C*H), 127.3 (Ar*C*H, 2C), 127.2 (Ar*C*H, 2C), 126.2 (Ar*C*H, 2C), 126.1 (Py*C*H), 126.0 (Ar*C*H, 2C), 119.2 (Py*C*H), 116.3 (Ar*C*), 116.1 (Ar*C*), 114.8 (Ar*C*H, 2C), 111.9 (PyCH), 100.7 (C≡C), 85.0 (C≡C), 77.9 (AlCH), 67.9 (AlCH), 56.3 (AlCH), 40.0 ($CH_2$), 23.3 ($CH_3$). **HRMS** (MALDI) (*m/z*) $[M+H]^+$ calculated for $C_{48}H_{35}N_4O_6$ 763.2557, found 763.2576.

**4-formyl-*N*-(6-methylpyridin-2-yl)benzamide Aldehyde**[5]

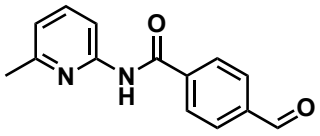

4-formylbenzoic acid (2.50 g, 16.7 mmol) in a mixture of $SOCl_2$/PhMe (60 mL, 2:1) was refluxed at 80 ˚C for 24 hours. The clear solution obtained was reduced under reduced pressure to yield the pure crude 4-formylbenzoyl chloride which was used in the next step without further purification (2.81 g, 100%).

**$^1$H NMR** (300.1 MHz, $CDCl_3$): $\delta_H$ 10.13 (s, 1H), 8.26 (d, *J* = 8.4 Hz, 2H), 8.00 (d, *J* = 8.4 Hz, 2H) **$^{13}$C NMR** (75.5 MHz, $CDCl_3$): $\delta_C$ 191.0 (*C*OH), 167.8 (*C*OCl), 140.5 (Ar*C*), 137.6 (Ar*C*), 131.8 (Ar*C*H, 2C), 129.8 (Ar*C*H, 2C).

Crude 4-formylbenzoyl chloride (2.80 g, 16.7 mmol) in dry $CH_2Cl_2$ (25 mL) under argon was slowly reacted with a solution of 6-methylpyridin-2-amine (1.81 g, 16.7 mmol) and $Et_3N$ (2.55 mL, 18.3 mmol) in dry $CH_2Cl_2$ (15 mL) at 0 ˚C. The reaction was left to stir for 48 hours at room temperature before being quenched with water (30 mL). The organic layer was washed with *aq*. HCl (1 M, 20 mL) and the combined aqueous layer was extracted with $CH_2Cl_2$ (3×40 mL). The combined organic layers were dried over $MgSO_4$, filtered and concentrated *in vacuo* to obtain a white solid. The crude product was purified by recrystallisation ($CH_2Cl_2$: Hexane, 100:1) to obtain the desired aldehyde as a white solid (2.51 g, 62%).

**M.p.**: 106.8-108.0 ˚C **$^1$H NMR** (500.1 MHz, $CDCl_3$): $\delta_H$ 10.06 (s, 1H), 9.03 (s, 1H), 8.15 (d, *J* = 8.2 Hz, 1H), 8.05-8.02 (m, 2H), 7.94-7.92 (m, 2H), 7.63 (dd, *J* = 8.1, 7.7 Hz, 1H), 6.91 (d, *J* = 7.4 Hz, 1H), 2.35 (s, 3H). **$^{13}$C NMR** (125.8 MHz, $CDCl_3$): $\delta_C$ 191.5 (*C*HO), 164.7 (*C*O), 157.1 (Py*C*), 150.6 (Py*C*), 139.5 (Ar*C*), 138.9 (Py*C*H), 138.6 (Ar*C*), 130.0 (Ar*C*H, 2C), 128.0 (Ar*C*H, 2C), 119.9 (Py*C*H), 111.3 (Py*C*H), 23.9 (*C*H$_3$). **HRMS** (EI+) (*m/z*) $[M+H]^+$ calculated for $C_{14}H_{13}N_2O_2$ 241.0972, found 241.0977.

**1-(p-tolyl)-1H-pyrrole-2,5-dione Control maleimide 4**[6]

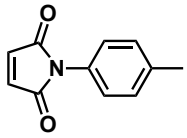

*p*-Toluidine (2.14 g, 20.0 mol) in acetic acid (50 mL) was reacted with maleic anhydride (1.96 g, 20.0 mmol) at room temperature for 3 hours. The yellow precipitate formed during the reaction was filtered, washed with $Et_2O$ (10 mL) and dried under vacuum to yield the uncyclised product in sufficient purity for direct conversion (2.52 g, 61%).

**M.p.**: 193.0-195.8 ˚C. **$^1$H NMR** (300.1 MHz, $d_6$-DMSO): $\delta_H$ 10.36 (s, 1H, COO*H*), 7.51 (d, *J* = 8.5 Hz, 2H), 7.13 (d, *J* = 8.1 Hz, 2H), 6.46 (d, *J* = 12.1 Hz, 1H), 6.30 (d, *J* = 12.1 Hz, 1H), 2.26 (s, 3H). **$^{13}$C NMR** (75.5 MHz, $d_6$-DMSO): $\delta_C$ 166.7 (*C*OOH), 163.0 (NH*C*O), 135.9 (Ar*C*), 133.0 (Ar*C*), 131.6 (=*C*H), 130.7 (=*C*H), 129.2 (Ar*C*H, 2C), 119.6 (Ar*C*H, 2C), 20.5 (*C*H$_3$). **MS** (EI–): m/z 203.89 (100%, $[M]^-$, 408.83 (62%), 204.95 (5%); **HRMS** (ES+): (*m/z*) $[M+Na]^+$ calculated for $C_{11}H_{11}NO_3Na$ 228.0631, found 228.0633.

$ZnBr_2$ (850 mg, 3.76 mmol) and hexamethyldisilazane (4 ml, 18.8 mmol) were added to a solution of (*Z*)-4-oxo-4-(p-tolylamino)but-2-enoic acid (771 mg, 3.76 mmol) in MeCN (40 mL). The reaction mixture was refluxed at 70 ˚C for one hour, before being quenched with water (50 mL). The organic layer was treated with conc. HCl (5 mL) and the aqueous layer was extracted with $CH_2Cl_2$ (3 × 200 mL). The combined organic layers were dried over $MgSO_4$, filtered and concentrated *in vacuo* to furnish the final control maleimide **4** as yellow solid (0.5 g, 71%).

**M.p.**: 148.2-151.2 ˚C. **$^1$H NMR** (500.1 MHz, $CDCl_3$): $\delta_H$ 7.28-7.26 (m, 2H), 7.22-7.19 (m, 2H), 6.84 (s, 2H), 2.38 (s, 3H). **$^{13}$C NMR** (125.8 MHz, $CDCl_3$): $\delta_C$ 169.8 (*C*O, 2C), 138.2 (Ar*C*), 134.3 (=*C*H, 2C), 129.9 (Ar*C*H, 2C), 128.6 (Ar*C*), 126.2 (Ar*C*H, 2C), 21.3 (*C*H$_3$). **MS** (CI+): m/z 188 (100, $[M+H]^+$); **HRMS** (CI+): (*m/z*) $[M+H]^+$ calculated for $C_{11}H_{10}NO_2$ 188.0706, found 188.0715.

### 3. Kinetic measurements by $^1$H NMR spectroscopy

NMR samples were prepared in a 5 mm NMR tube (Wilmad 528PP) by mixing appropriate volumes of stock solutions such that the total volume was 0.8 mL and the concentration of each component was 10 mM. A polyethylene pressure cap was then applied to the top of the tube to prevent solvent evaporation. The NMR tube was transferred to the NMR spectrometer (Varian UNITYplus) regulated at the desired temperature, and 500.1 MHz $^1$H NMR spectra were acquired automatically at a given time interval over a period of 5 to 16 hours. Analysis and deconvolution of the arrayed set of $^1$H NMR spectra recorded during this time was performed using iNMR software (Version 5.4.7, Mestrelab Research, 2015).

The chemical reaction monitored in the described systems was a 1,3-dipolar cycloaddition between a maleimide and a nitrone, giving rise to two cycloadduct products. The percentage completion of the reaction was monitored through the disappearance of the signal arising from the maleimide protons and the appearance of the signal corresponding to the cycloadduct protons. The diastereoisomeric products of the reaction between a nitrone and a maleimide are easily distinguishable in the $^1$H NMR spectrum (**Figure S1**). The signals arising from the isoxazolidine protons give a different splitting pattern for the *cis* and *trans* cycloadducts.

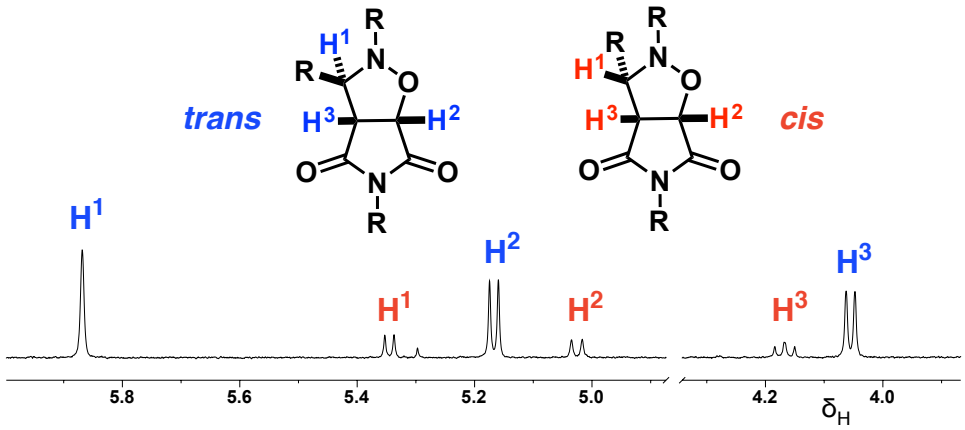


**Fig. S1** Partial $^1$H NMR spectrum (500.1 MHz, $CDCl_3$) featuring the characteristic splitting pattern for the *trans* (blue) and *cis* (red) cycloadducts. The *trans* diastereoisomer exhibits a singlet ($H^1$) and to doublets ($H^2$ and $H^3$), while the *cis* diastereoisomer presents as two doublets ($H^1$ and $H^2$) and a doublet of doublets ($H^3$). The diastereoisomeric products shown were formed by the reaction of nitrone **1b** with control recognition-disabled maleimide **4** (10 mM in $CDCl_3$ at 0 °C).

In order to extract product concentrations from the $^{1}$H NMR data, the area of the signal arising from the maleimide protons and one of the signals of the corresponding cycloadduct protons was calculated through deconvolution of the spectra. The area of the maleimide protons signal was divided by two and added to the area of the cycloadduct proton signal. The obtained number signifies the area of a proton signal of a species at a concentration of 10 mM and was used as a reference to calculate the concentration of all species detectable in the spectrum. This procedure was repeated for all spectra recorded at different time points. The time at which each spectrum was recorded was extracted from the log file, which accompanies the NMR spectroscopy data. Knowing the concentration of the products at each time point, it was possible to plot a reaction profile for each reaction using the proFit program (version 6.2.9, Quantum Soft, Switzerland). Rate data ($d$[product]/$d$t) for each kinetic experiment were determined by computing the first derivative of a seventh-order polynomial fitted to the concentration *vs* time data.

**Figure S2** shows the kinetic concentration *vs* time profile for the reaction between the nitrone **1b** and maleimide **2** (10 mM in $CDCl_3$) as determined by means of $^{1}$H NMR (500 MHz, 0 ˚C). The reaction profile (**Figure S2a**) shows the typical sigmoidal shape, characteristic for a self-replicating system, with a short lag period. The 1,3-dipolar cycloaddition proceeded with high diastereoselectivity, reaching over 80% to the *trans*-**3b** product after 7.3 hours (no *cis* diastereoisomer was detected). The maximum rate of the reaction is reached after *ca*. 100 minutes (**Figure S2b**).

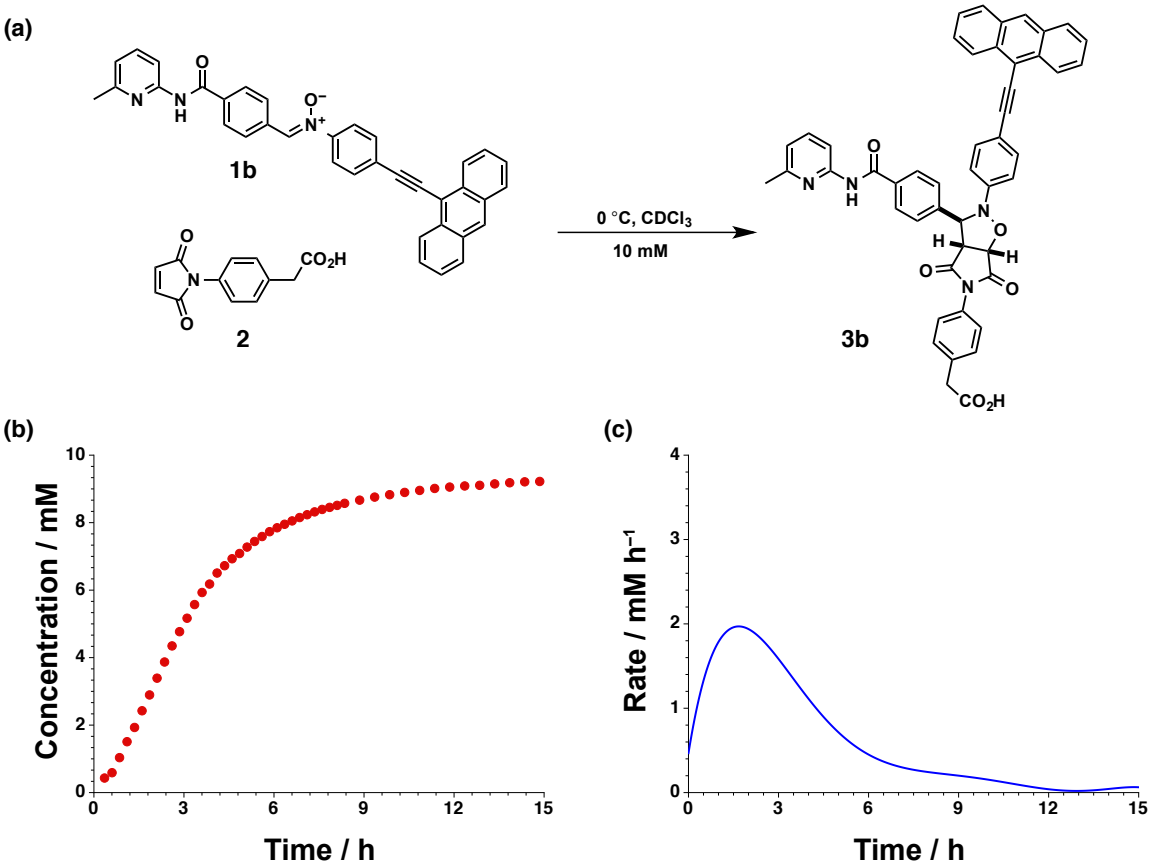


**Fig. S2** **(a)** Reaction between nitrone **1b** and maleimide **2** affords the *trans*-**3b** cycloadduct exclusively. **(b)** The concentration *vs* time profile for the formation of the *trans* (•) product (10 mM in $CDCl_3$ at 0 ˚C, no *cis* product was observed). **(c)** Rate *vs* time profile for the formation of the *trans* diastereoisomer (•).

Reaction of the nitrone **1b** and maleimide **2** was examined in the presence of 10 mol% of preformed *trans*-**3b** as template. **Figure S3a** shows the concentration *vs* time profile for the template instructed reaction, showing a clear disappearance of the lag period, with a decrease in the time required to reach the maximum reaction rate to 36 min, as shown in **Figure S3b**.

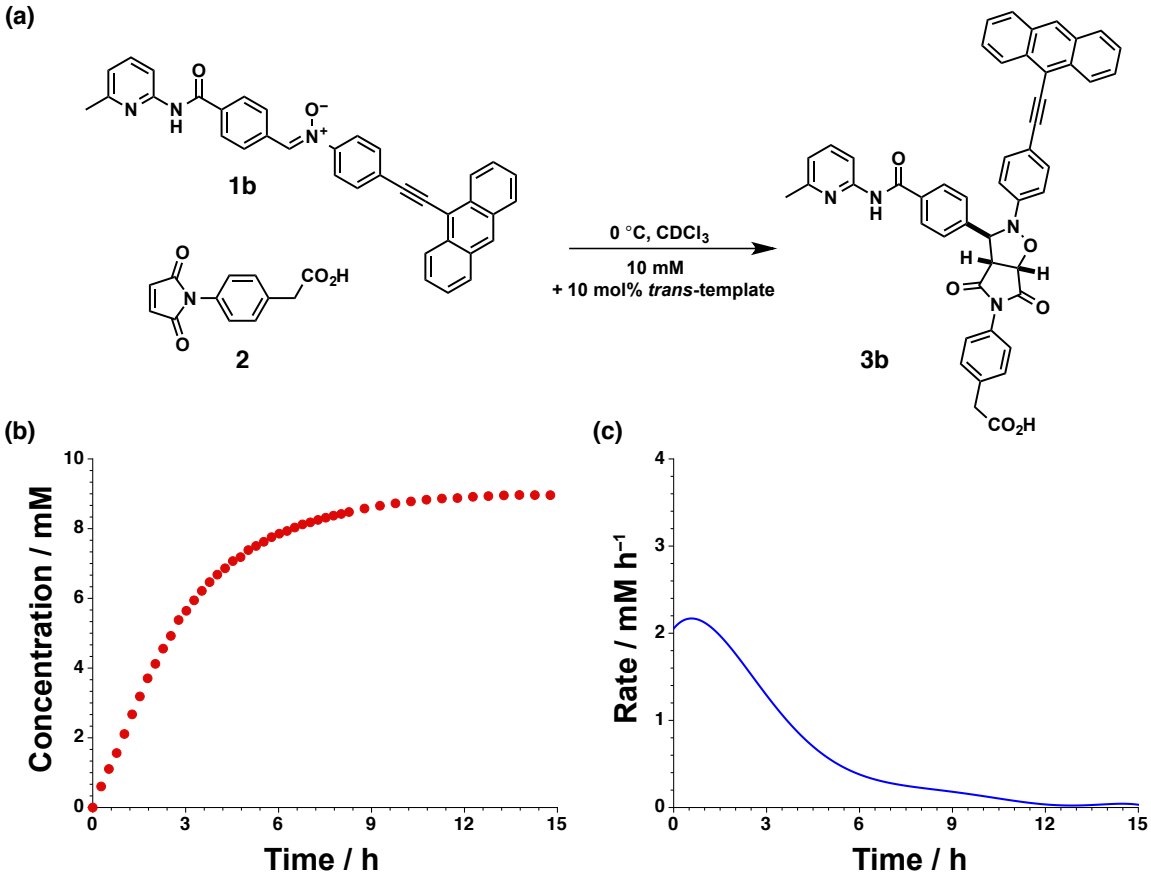


**Fig. S3** **(a)** Reaction between nitrone **1b** and maleimide **2** in the presence of 10 mol% pre-formed *trans*-**3b** template. **(b)** The concentration *vs* time profile for the formation of *trans*-**3b** (•) product (10 mM in $CDCl_3$ at 0 ˚C, no *cis* product was observed). **(c)** Rate *vs* time profile for the formation of the *trans* diastereoisomer (•).

In order to confirm the reliance of the replicating system on the recognition-mediated processes, the reaction between the nitrone **1b** and control *p*-Me substituted maleimide **4**, which does not possess the phenylacetic acid recognition group, was examined. The concentration *vs* time profile shows that the reaction is slow and unselective (**Figure S4**), resulting in formation of both diastereoisomeric products *trans*-**5b** and *cis*-**5b**.

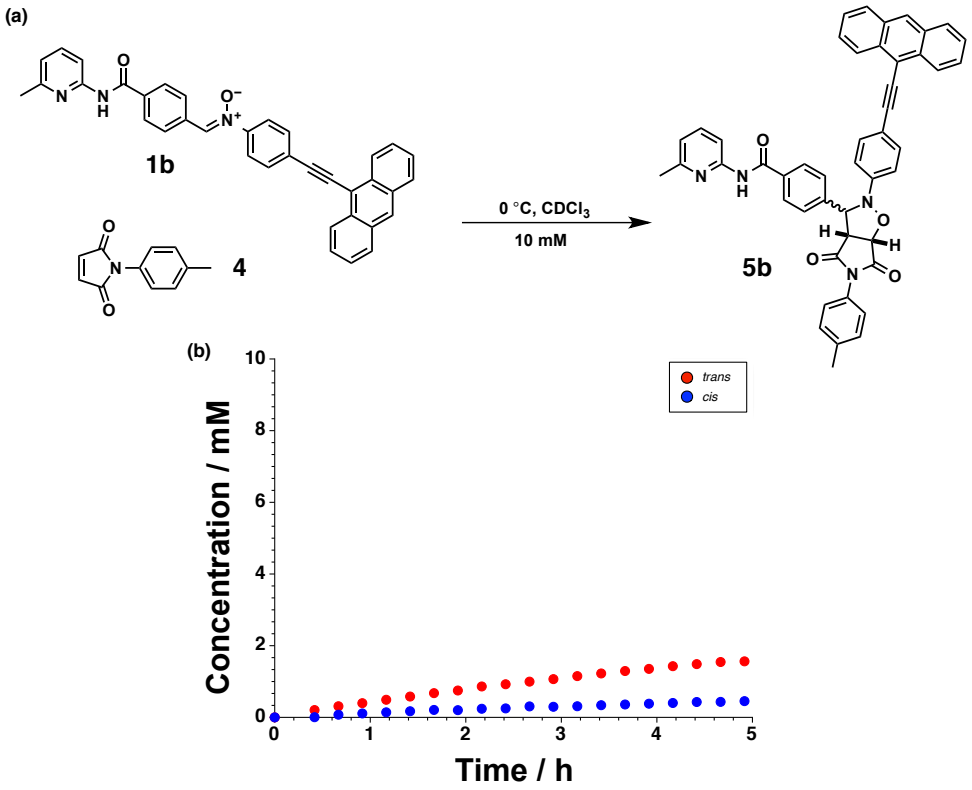


**Fig. S4** **(a)** Reaction between nitrone **1b** and maleimide **4** gives rise to two diasteroisomeric cycloadducts, *cis*-**5b** and *trans*-**5b**. **(b)** The concentration *vs* time profile for the formation of *trans*-**5b** (•) and *cis*-**5b** products (•) (10 mM in $CDCl_3$ at 0 ˚C).

**4. Kinetic measurements by UV-Vis spectroscopy**

A Perkin Elmer Lambda 35 UV/VIS spectrometer was used to collect the UV-Vis spectra. The reaction was run by mixing appropriate volumes of reagent solutions to obtain a 5 mL stock solution of total reagent concentration at 10 mM in $CHCl_3$. 6 μL of the stock solution were withdrawn at various time points during the reaction and diluted to give a total volume of 1.50 mL $CHCl_3$ solution. These solutions were analyzed instantly in the spectrometer using cuvettes with optical path of 0.5 cm, scanning in the 600-200 nm range. The absorbance corresponding to the maxima of increasing and decreasing bands were plotted against the sampling time to generate the kinetic curves for the progression of the reaction.

## 5. Kinetic measurements by fluorescence spectroscopy

A Cary Eclipse spectrofluorimeter (Varian Inc., Palo Alto, USA) was used to collect the emission spectra. A cuvette with an optical path of 0.2 cm was filled with a 10 mM solution of reagents in $CHCl_3$. Spectra were acquired automatically every 0.6 seconds for a period of five hours.

The variation of nitrone concentration was followed by excitation at 459 nm and collecting the light at 549 nm, while the formation of product was followed by excitation at 430 nm and collecting the light at 470 nm. The exciting beams were sent alternatively with a time delay of 0.5 s through a 10 mM solution of nitrone **1b** and maleimide **2** in $CHCl_3$. **Figure S5** shows the intensity of the light emitted by the nitrone and the cycloadduct **3** plotted *vs* time.

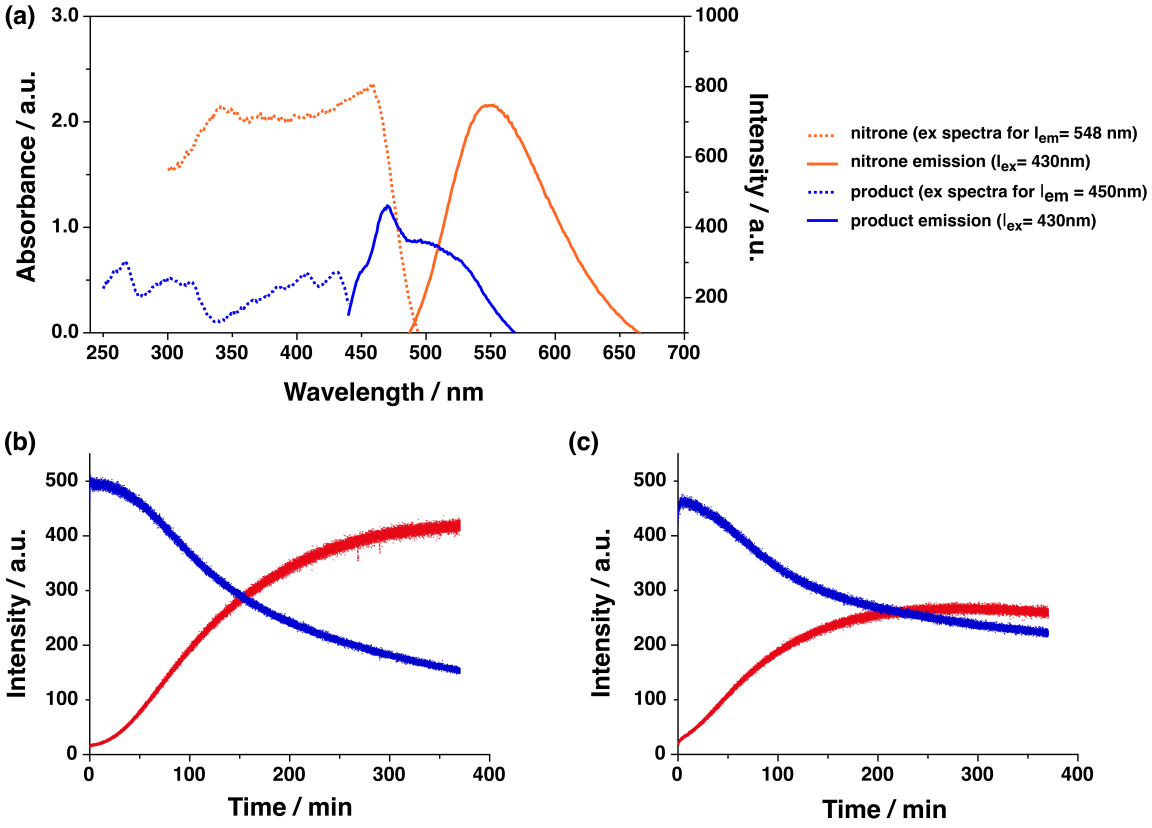


**Figure S5** **(a)** Excitation (dotted line) and emission (full line) spectra of 10 mM solution of nitrone **1b** (**orange**) and cycloadduct **3** (**blue**). **(b)** Profile of intensity of light emitted at 549 nm (corresponding to nitrone **1b** emission) and at 470 nm (corresponding to cycloadduct **3** emission) with respect to the time of reaction (10 mM starting material solution in $CHCl_3$, 20 °C); **(c)** Intensity *vs* time profile of the reaction after addition of 10 mol% of template *trans*-**3b** at the start of the reaction.

Both curves are S-shaped, confirming again the formation of cycloadduct through an autocatalytic mechanism. In this case the lag period at the beginning of the reaction is longer. This could be due to the overlap between the emission bands of the product with the excitation band of the nitrone.

## 6. Kinetic simulations and fitting

All kinetic fitting and simulations were performed using the software package SimFit[7] (Günter von Kiedrowski, 2008) and the ISOSIM mode incorporated within the SimFit package. A detailed kinetic model of all possible interactions involved in the studied systems was constructed (example for the self-replicating reaction is attached in **Section 10**). This model was converted into a series of rate equations whose solution determine the concentration of reactant and product species as a function of time. The program varies experimentally inaccessible kinetic values until the calculation matches the experimental data. The fitting was performed for the concentration *vs* time data obtained for the reaction of nitrone **1b** with maleimide **2** at 20 °C. Overview of the kinetic parameters obtained from this fitting procedure is shown in **Table S1**.

**Table S1** Kinetic and association parameters obtained for the reaction of nitrone **1b** and maleimide **2** (10 mM, $CDCl_3$, 20 °C) by kinetic fitting of the experimental data using SimFit simulation and software package (Günter von Kiedrowski, University of Bochum, 2008).

| | *trans*-**3b** | *cis*-**3b** |
|---|---|---|
| $k_{bimolecular}$ / $10^{-3}$ $M^{-1}s^{-1}$ | 1.72 | 0.568 |
| $k_{unimolecular}$ / $10^{-3}$ $s^{-1}$ | 27.9 | 0.0179 |
| **Effective Molarity** / M | 16.2 | 0.0315 |
| $K_a$ **Duplex** / $10^5$ $M^{-1}$ | 3.74 | – |
| **RMS%** | 0.394 | |

This data was then used to construct a simulation of the UV-Vis kinetic curve. Specifically, the simulation utilized the concentrations of nitrone ($c_n$) and template ($c_t$) at

$$A_\lambda = A_n + A_t = b(\varepsilon_n c_n + \varepsilon_t c_t)$$

different times extracted from the $^1$H NMR kinetic experiment (20 °C, $CDCl_3$). These concentrations were used to calculate the total absorbance at wavelength λ ($A_\lambda$), which is obtained by the sum of absorbance of nitrone ($A_n$) and template ($A_t$) by the formula where $\varepsilon_n$ and $\varepsilon_t$ are the molar absorbance coefficients of nitrone and template at wavelength λ. Plotting the total absorbance against the time of the NMR measurement, a kinetic curve can be obtained and compared with the measured UV-Vis kinetic curve (**Figure 2**, main manuscript).

## 7. Wave diffusion analysis

A 5 mM solution of reagents was transferred into two 50 μL glass syringes. Approximately 2 μL of a 10 mM solution of pre-formed template **3b** were taken up very slowly to create a "template seed" region on the top of the first syringe. A UV lamp (λ = 365 nm) was placed over the syringes. In order to compare the mechanism of the self-replicating wave with the effect of exclusive diffusion, the same amount of template was simultaneously added to a syringe solely containing 5 mM solution of nitrone. Pictures of the syringes were taken every two minutes, using a Samsung PL50 camera with an exposure value of –2 and the white balance settled for fluorescence light. The experiment was run at room temperature (20 ˚C). No self-replicating wave was observed during the control experiment.

### 7.1 Data processing of the propagating reaction-diffusion front images

Color images were collected every 2 minutes during the duration of the experiment using a Samsung PL50 camera and were opened in the image processing package Fiji (http://fiji.sc/) and were batch processed according to the following protocol. Each image had auto level correction applied, was cropped to the area of interest (the first 15 μL of the syringe), and the RGB channels were manipulated to remove the yellow color arising from nitrone **1b**. These batch processed images were exported in as 8 bit grayscale TIFFs and the compiled sequence provided a clear time-lapse overview of the reaction-diffusion front progress (Figure 4a, main manuscript).

Profiling of the 8 bit grayscale images (**Figure 4b**, main manuscript) was also accomplished using Fiji using the Plot Profile command. These profiles were used to measure a front propagation by applying a running average function to the data to remove the effect of the vertical black lines (volume marks on the syringe) visible over the reaction-diffusion front.

## 8. Computational methods

### 8.1 Estimation of UV-Vis spectra for nitrone 1b and replicator 3b

Geometry optimizations and TD-DFT calculations were performed using the Gaussian09[8] suite of programs –revision D.01 was used in all calculations. Calculations were performed using the B3LYP[9] functional and the 6-311+G(2d,p) basis set. The geometries of nitrone **6** and cycloadduct **7** – used as models for nitrone **1b** and replicator **3b** respectively – were optimized fully in internal (keyword: `opt`) or cartesian (keyword: `opt=cartesian`) coordinates using the default optimisation protocols within Gaussian09. Stationary points were characterized by means of a vibrational analysis (keyword: `freq`).

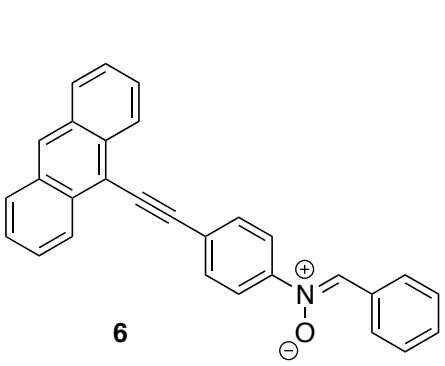


**6**

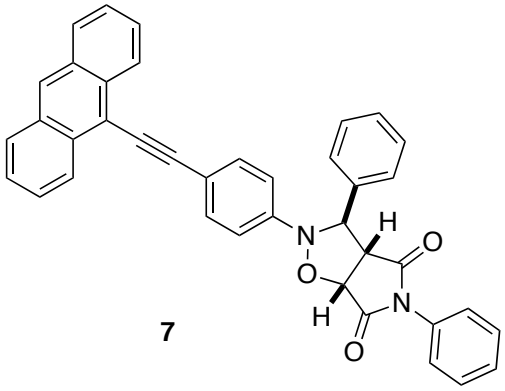


**7**

UV-Vis spectra were calculated using TD-DFT as implemented in Gaussian09 and 12 singlet excited states (keyword: `td=singlet,NStates=12`) were calculated for compounds **6** and **7**. Spectra (**Figure S6**) were created from the Gaussian output using Chemissian (http://www.chemissian.com/, Version 4.38) and the same program was used to compute the NTOs associated with each transition. The calculations reveal (**Figure S6**) an absorption band at 393 nm in nitrone **6** that is associated with either HOMO–1 to LUMO or HOMO to LUMO+1 excitation that is entirely absent in the spectrum of cycloadduct **7**.

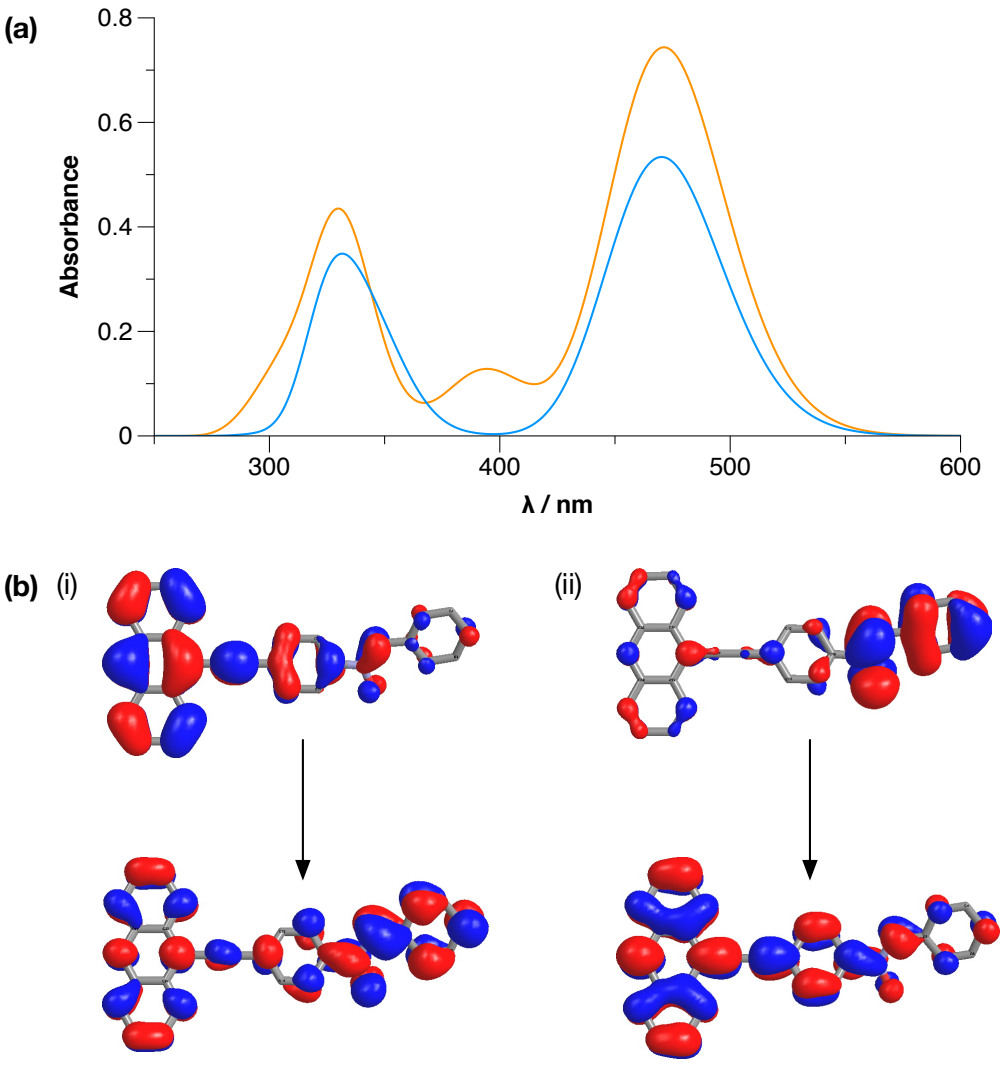


**Figure S6** (a) Calculated UV-Vis spectra for nitrone **6** (orange) and cycloadduct **7** (blue). (b) Calculated NTOs for nitrone **6** (i) HOMO to LUMO+1 and (ii) HOMO–1 to LUMO

### 8.2 Transition state for the formation of replicator 3b within the [1b•2•3b] complex

An initial transition state guess was generated by grid scan extension within the [**3b•3b**] dimer of the C—O and C—C bonds that are formed during the cycloaddition reaction. The structure of this approximate transition state was then relaxed using a constrained optimization that held the lengths of the partial C–C and C–O associated with the transition state fixed while allowing all other coordinates to vary. Vibrational analysis of this structure was then used to instruct a full optimization that located the transition state for the cycloaddition. The identity of the transition state was confirmed by vibrational

analysis that demonstrated that the structure located possessed one imaginary frequency ($\nu_i = -673$ cm$^{-1}$) corresponding to the reaction coordinate of the cycloaddition reaction. All calculations were performed at the RM1 level of theory using either MOPAC2016[10] (Version 16.057M) or GAMESS[11] (the version dated 5 December 2014, compiled from source using gfortran 5.3.0 and the Apple Accelerate math library, was used in all calculations).

## 9. References


(1) Maleimide **2** was prepared from maleic anhydride and 4-aminophenylacetic acid using an adapted version of the procedure reported in Kassianidis, E.; and Philp, D. *Angew. Chem. Int. Ed.* **2006**, *45*, 6344.

(2) Heuft, M. A.; Collins, S. K.; Yap, G. P. A.; Fallis, A. G. *Org. Lett.*, **2001**, *3*, 2883.

(3) Nierth, A.; Kobitski, A. Y.; Nienhaus, G. U.; and Jäschke, A. *J. Am. Chem. Soc.*, **2010**, *132*, 2646.

(4) Akiyama, S.; Tajima, K.; Nakatsuji, S.; Nakashima, K.; Abiru, K.; Watanabe, M. *Bull. Chem. Soc. Jpn.*, **1995**, *68*, 2043.

(5) Kassianidis, E.; Philp, D. *Angew. Chem. Int. Ed.* **2006**, *45*, 6344.

(6) Thamizharasi, S.; Reddy, B. S. R. *J. Appl. Polym. Sci.* **2001**, *80*, 1870.

(7) Sievers, D.; von Kiedrowski, G. *Chem. Eur. J.* **1998**, *4*, 629.

(8) Gaussian 09, Revision D.01, Frisch, M. J.; Trucks, G. W.; Schlegel, H. B.; Scuseria, G. E.; Robb, M. A.; Cheeseman, J. R.; Scalmani, G.; Barone, V.; Mennucci, B.; Petersson, G. A.; Nakatsuji, H.; Caricato, M.; Li, X.; Hratchian, H. P.; Izmaylov, A. F.; Bloino, J.; Zheng, G.; Sonnenberg, J. L.; Hada, M.; Ehara, M.; Toyota, K.; Fukuda, R.; Hasegawa, J.; Ishida, M.; Nakajima, T.; Honda, Y.; Kitao, O.; Nakai, H.; Vreven, T.; Montgomery, J. A.; Peralta, Jr., J. E.; Ogliaro, F.; Bearpark, M.; Heyd, J. J.; Brothers, E.; Kudin, K. N.; Staroverov, V. N.; Kobayashi, R.; Normand, J.; Raghavachari, K.; Rendell, A.; Burant, J. C.; Iyengar, S. S.; Tomasi, J.; Cossi, M.; Rega, N.; Millam, J. M.; Klene, M.; Knox, J. E.; Cross, J. B.; Bakken, V.; Adamo, C.; Jaramillo, J.; Gomperts, R.; Stratmann, R. E.; Yazyev, O.; Austin, A. J.; Cammi, R.; Pomelli, C.; Ochterski, J. W.; Martin, R. L.; Morokuma, K.; Zakrzewski, V. G.; Voth, G. A.; Salvador, P.; Dannenberg, J. J.; Dapprich, S.; Daniels, A. D.; Farkas, Ö.; Foresman, J. B.; Ortiz, J. V.; Cioslowski, J.; Fox, D. J. Gaussian, Inc., Wallingford CT, **2009**.

(9) Becke, A. D. *J. Chem. Phys*., **1993**, *98*, 5648.

(10) MOPAC2016, James J. P. Stewart, Stewart Computational Chemistry, Colorado Springs, CO, USA, HTTP://OpenMOPAC.net (**2016**)

(11) (a) Schmidt, M. W.; Baldridge, K. K.; Boatz, J. A.; Elbert, S. T.; Gordon, M. S.; Jensen, J. H.; Koseki, S.; Matsunaga, N.; Nguyen, K. A.; Su, S. J.; Windus, T. L.; Dupuis, M.; Montgomery, J. A. *J. Comput. Chem.* **1993**, *14*, 1347. (b) "Advances in electronic structure theory: GAMESS a decade later" Gordon, M. S.; Schmidt, M. W. Chapter 41, pp 1167-1189, in "Theory and Applications of Computational Chemistry, the first forty years" Dykstra, C. E.; Frenking, G.; Kim, K. S.; Scuseria, G. E.Eds.; Elsevier, Amsterdam, **2005**.

## 10. Kinetic script

```
*============================================================
* phenylacetic acid Maleimide 2 + anthracene Nitrone 1b to make replicator 3b
*============================================================
* all components at 10 mM, at 20 C
* A is maleimide 2
* B is nitrone 1b
* TRANS is the template 3b observed. No cis-3b was observed experimentally
*============================================================

DIM (4)

* Bimolecular routes to TRANS
REACTION (A + B        --> TRANS      )     CONSTANT ( 1, 1E-4, 1, 1, 100)

* Bimolecular routes to CIS
REACTION (A + B        --> CIS        )     CONSTANT ( 2, 1E-4, 1, 0.33, 100)

* Formation of binary complexes including product duplexes
* Only [TRANS*TRANS] is stable beyond one Pyr*COOH association

REACTION (A + TRANS    ==> ATRANS     )     CONSTANT ( 3, 1E9, 0) CONSTANT ( 4, 3E+6, 0)
REACTION (B + TRANS    ==> BTRANS     )     CONSTANT ( 5, 1E9, 0) CONSTANT ( 6, 3E+6, 0)
REACTION (A + BTRANS   ==> ABTRANS    )     CONSTANT ( 7, 1E9, 0) CONSTANT ( 8, 3E+6, 0)
REACTION (B + ATRANS   ==> ABTRANS    )     CONSTANT ( 9, 1E9, 0) CONSTANT (10, 3E+6, 0)
REACTION (A + CIS      ==> ACIS       )     CONSTANT (11, 1E9, 0) CONSTANT (12, 3E+6, 0)
REACTION (B + CIS      ==> BCIS       )     CONSTANT (13, 1E9, 0) CONSTANT (14, 3E+6, 0)
REACTION (A + BCIS     ==> ABCIS      )     CONSTANT (15, 1E9, 0) CONSTANT (16, 3E+6, 0)
REACTION (B + ACIS     ==> ABCIS      )     CONSTANT (17, 1E9, 0) CONSTANT (18, 3E+6, 0)
REACTION (TRANS + TRANS==> TRANSTRANS )     CONSTANT (19, 1E9, 0)
                                            CONSTANT (20, 1.00E+3, 2, 1, 100)
REACTION (CIS  + CIS   ==> CISCIS     )     CONSTANT (21, 1E9, 0) CONSTANT (22, 3E+6, 0)
REACTION (TRANS + CIS  ==> TRANSCIS   )     CONSTANT (23, 1E9, 0) CONSTANT (24, 3E+6, 0)
REACTION (A + B        ==> AB         )     CONSTANT (25, 1E9, 0) CONSTANT (26, 3E+6, 0)

* Ternary complex reaction
REACTION (ABTRANS      --> TRANSTRANS )     CONSTANT (27, 1E-2, 3, 1, 100)

*Bimolecular Reactions of Complexes

REACTION (AB + A       --> TRANS + A             )      CONSTANT (28, 1E-4, 1, 1, 100)
REACTION (AB + B       --> TRANS + B             )      CONSTANT (29, 1E-4, 1, 1, 100)
REACTION (AB + A       --> CIS + A               )      CONSTANT (30, 1E-4, 1, 0.33, 100)
REACTION (AB + B       --> CIS + B               )      CONSTANT (31, 1E-4, 1, 0.33, 100)

REACTION (AB + ACIS    --> TRANS + A + CIS       )      CONSTANT (32, 1E-4, 1, 1, 100)
REACTION (AB + BCIS    --> TRANS + B + CIS       )      CONSTANT (33, 1E-4, 1, 1, 100)
REACTION (AB + ATRANS  --> TRANS + A + TRANS     )      CONSTANT (34, 1E-4, 1, 1, 100)
REACTION (AB + BTRANS  --> TRANS + B + TRANS     )      CONSTANT (35, 1E-4, 1, 1, 100)

REACTION (AB + ACIS    --> CIS  + A + CIS        )      CONSTANT (36, 1E-4, 1, 0.33, 100)
REACTION (AB + BCIS    --> CIS  + B + CIS        )      CONSTANT (37, 1E-4, 1, 0.33, 100)
REACTION (AB + ATRANS  --> CIS  + A + TRANS      )      CONSTANT (38, 1E-4, 1, 0.33, 100)
REACTION (AB + BTRANS  --> CIS  + B + TRANS      )      CONSTANT (39, 1E-4, 1, 0.33, 100)

REACTION (AB + ABCIS   --> CIS  + A + B + CIS    )      CONSTANT (40, 1E-4, 1, 0.33, 100)
REACTION (AB + ABCIS   --> TRANS + A + B + CIS   )      CONSTANT (41, 1E-4, 1, 1, 100)
REACTION (AB + ABTRANS --> CIS  + A + B + TRANS  )      CONSTANT (42, 1E-4, 1, 0.33, 100)
REACTION (AB + ABTRANS --> TRANS + A + B + TRANS )      CONSTANT (43, 1E-4, 1, 1, 100)

REACTION (       2 AB  --> TRANS + A + B         )      CONSTANT (44, 1E-4, 1, 1, 100)
REACTION (       2 AB  --> CIS  + A + B          )      CONSTANT (45, 1E-4, 1, 0.33, 100)

REACTION (         AB  --> CIS                   )      CONSTANT (46, 1.0E-5, 4, 1, 100)

REACTION ( COMPILE )

REACTION ( SHOW    )
CONSTANT ( SHOW    )
```

```
DEFINE   ( 1, TRANS , P, 1) SCALE (3,1)
DEFINE   ( 2, CIS   , P, 5) SCALE (3,1)

SELECT   ( TRANS, CIS  )

READ     ( TKIB_01     )

REACTION ( DOC         )
CONSTANT ( DOC         )

TIME     ( SEC         )

WIN      ( 0, 20000, 15000, 200, 0, 10e-3, 2e-3, 3e-4)

ASSIGN   ( OBS,  TRANS = TRANS + ATRANS + BTRANS + ABTRANS + 2 TRANSTRANS + TRANSCIS )
ASSIGN   ( OBS,  A     = A     + AB     + ATRANS + ABTRANS + ACIS         + ABCIS    )
ASSIGN   ( OBS,  CIS   = CIS   + ACIS   + ABCIS  + BCIS    + 2 CISIS      + TRANSCIS )

ASSIGN   ( SPEC, A     = #10E-3 )
ASSIGN   ( SPEC, B     = #10E-3 )
ASSIGN   ( SPEC, TRANS = TRANS )
ASSIGN   ( SPEC, CIS   = CIS   )

CHOOSE   ( EXP1 )
OPAR     ( 1E24 )
INTEG    (STIFF, 1E-11, 50, 0.025, 100, 50)
PLOT     (OBS, RES)

* Optimise rate constant using simplex

SIMPLEX  (PLOT)
SIMPLEX  (PLOT)
SIMPLEX  (PLOT)
SIMPLEX  (PLOT)
SIMPLEX  (PLOT)
SIMPLEX  (PLOT)
NEWTON   (PLOT)

PLOT     ( FILE )
PLOT     (OBS, RES)
```

## 11. NMR spectroscopic data

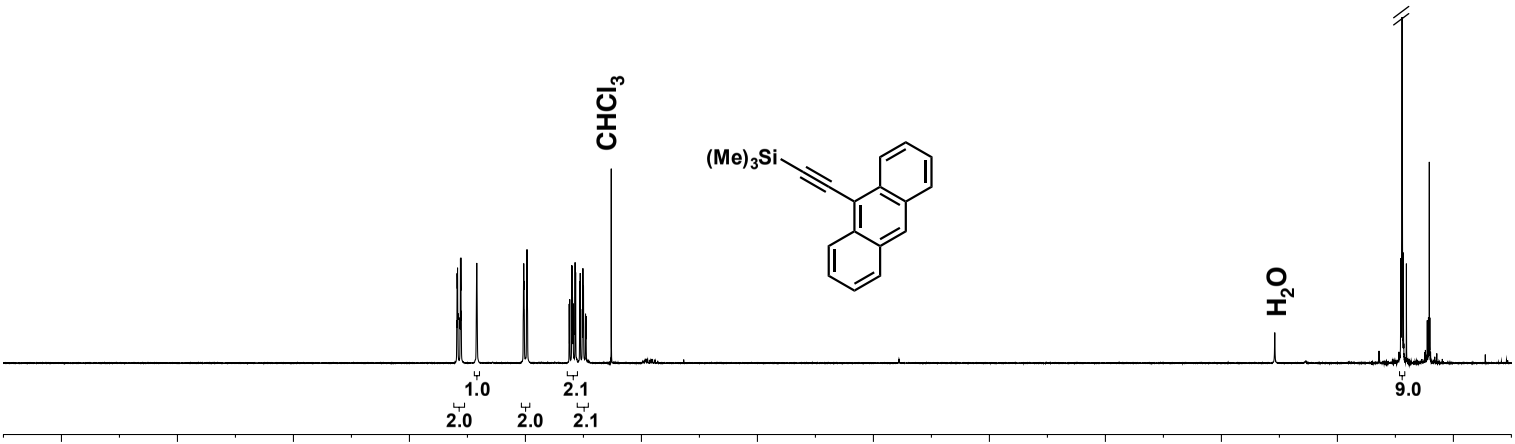


$^{1}$H NMR spectrum (300.1 MHz, RT, $CDCl_3$) of TMS protected compound

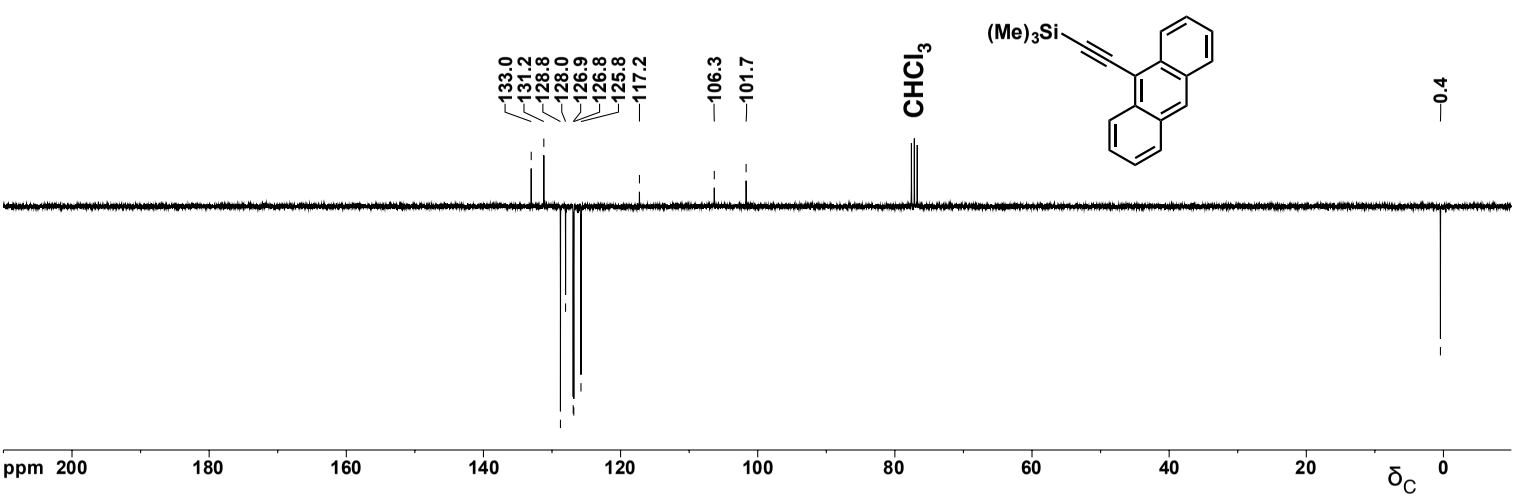


$^{13}$C NMR spectrum (75.5 MHz, RT, $CDCl_3$) of TMS protected compound

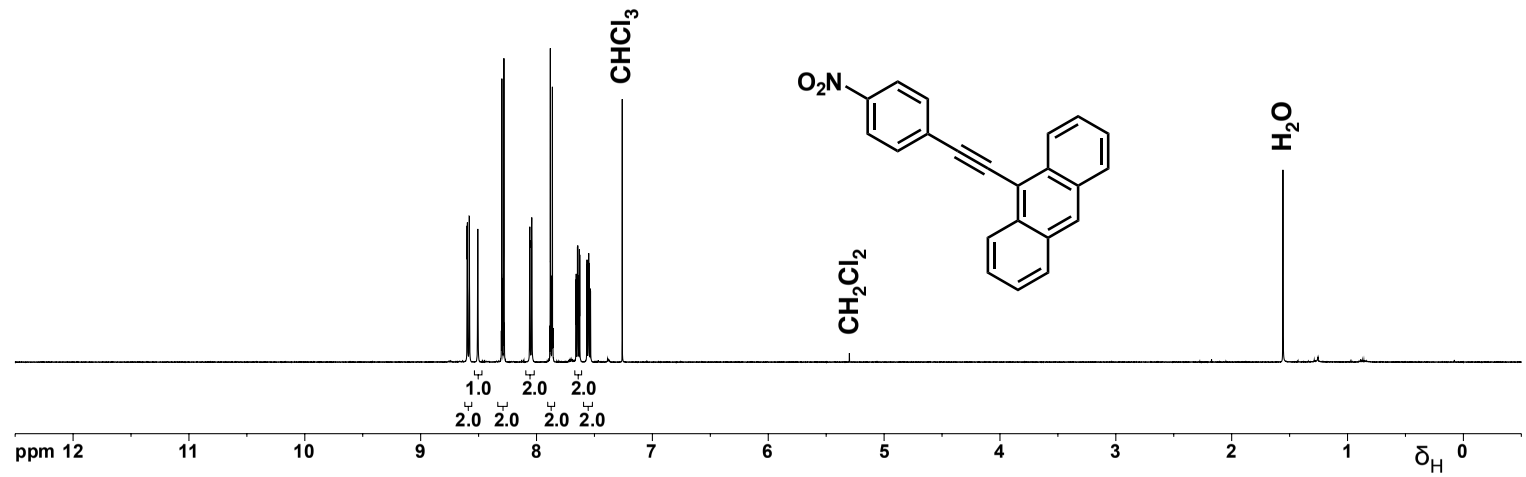


$^{1}$H NMR spectrum (500.1 MHz, RT, $CDCl_3$) of nitro compound

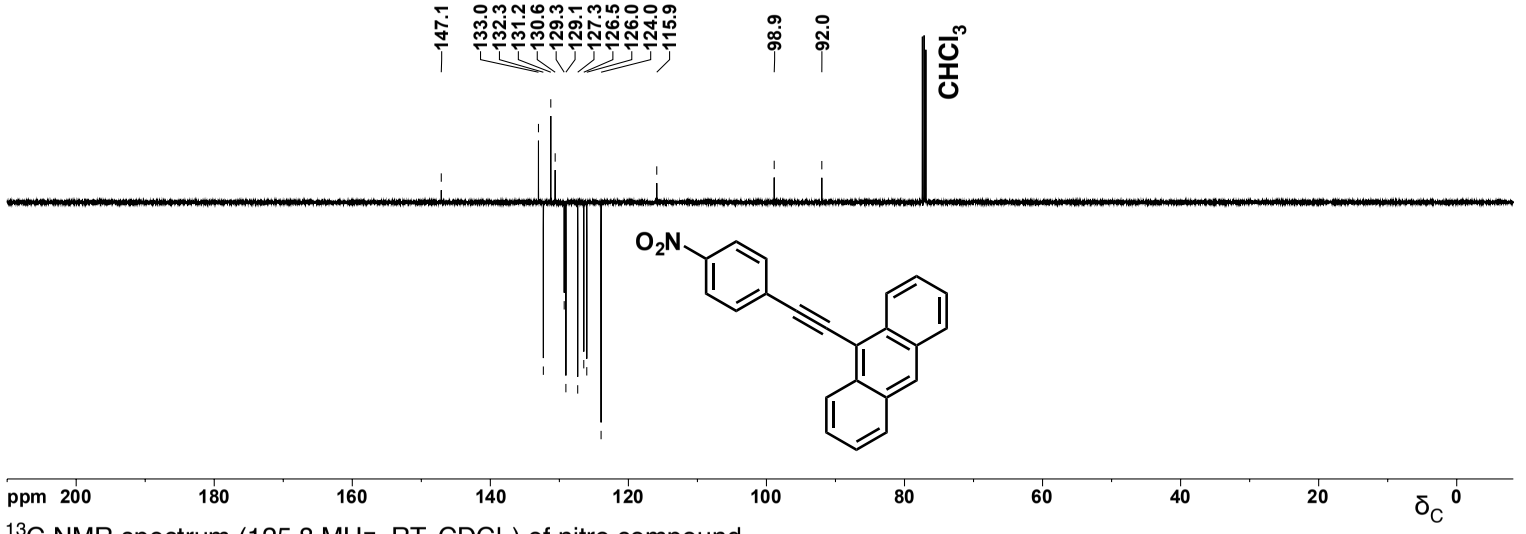


$^{13}$C NMR spectrum (125.8 MHz, RT, $CDCl_3$) of nitro compound

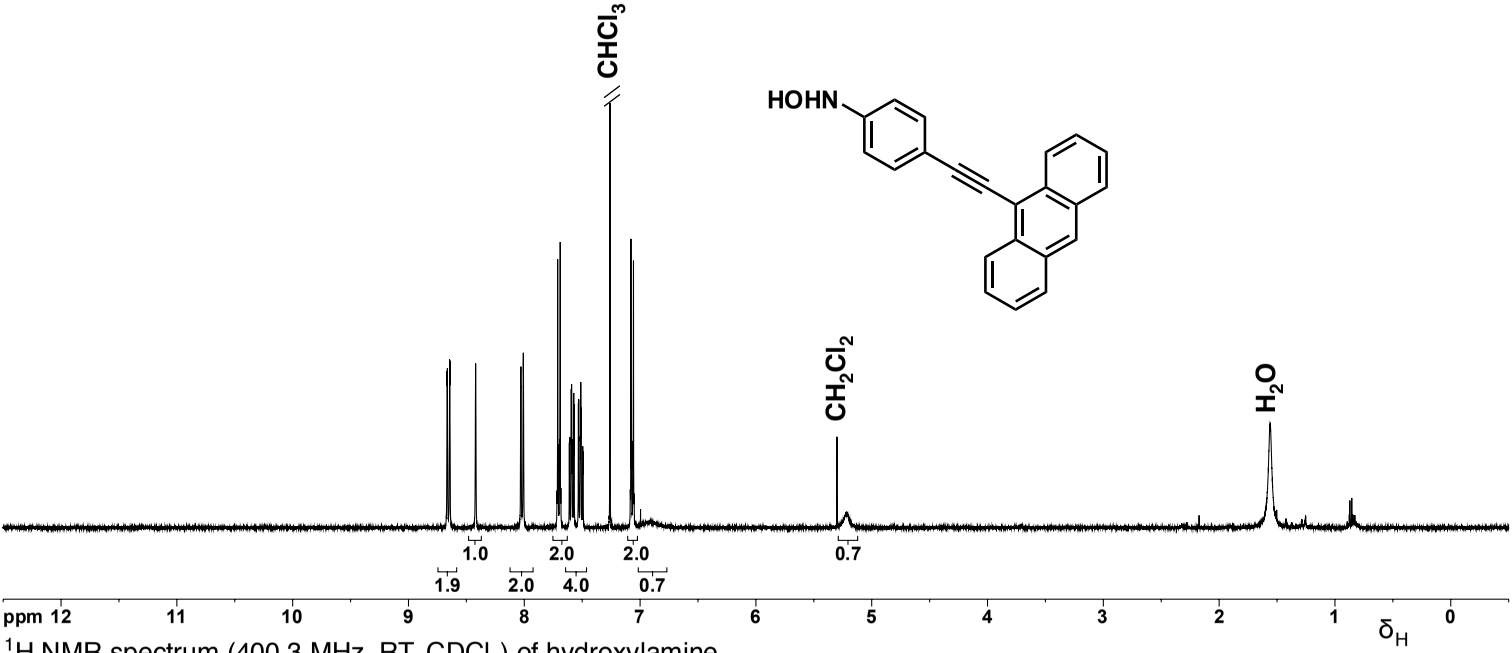


$^{1}$H NMR spectrum (400.3 MHz, RT, $CDCl_3$) of hydroxylamine

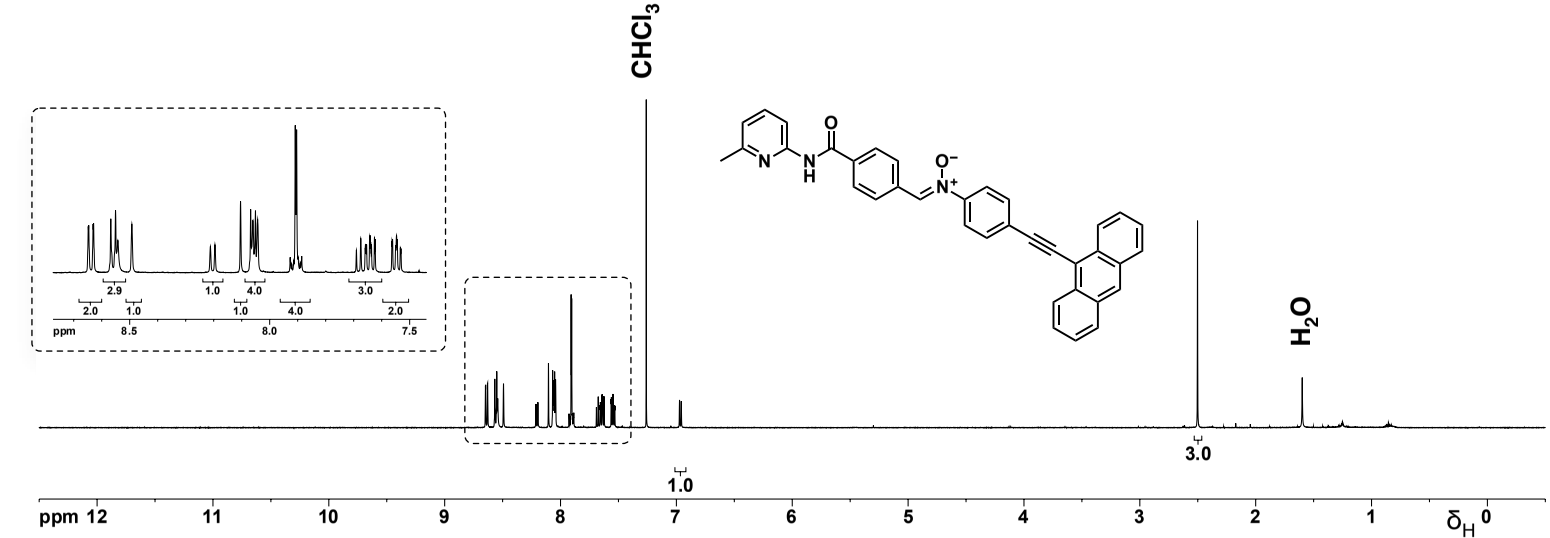


$^1$H NMR spectrum (500.1 MHz, RT, $CDCl_3$) of nitrone **1b**

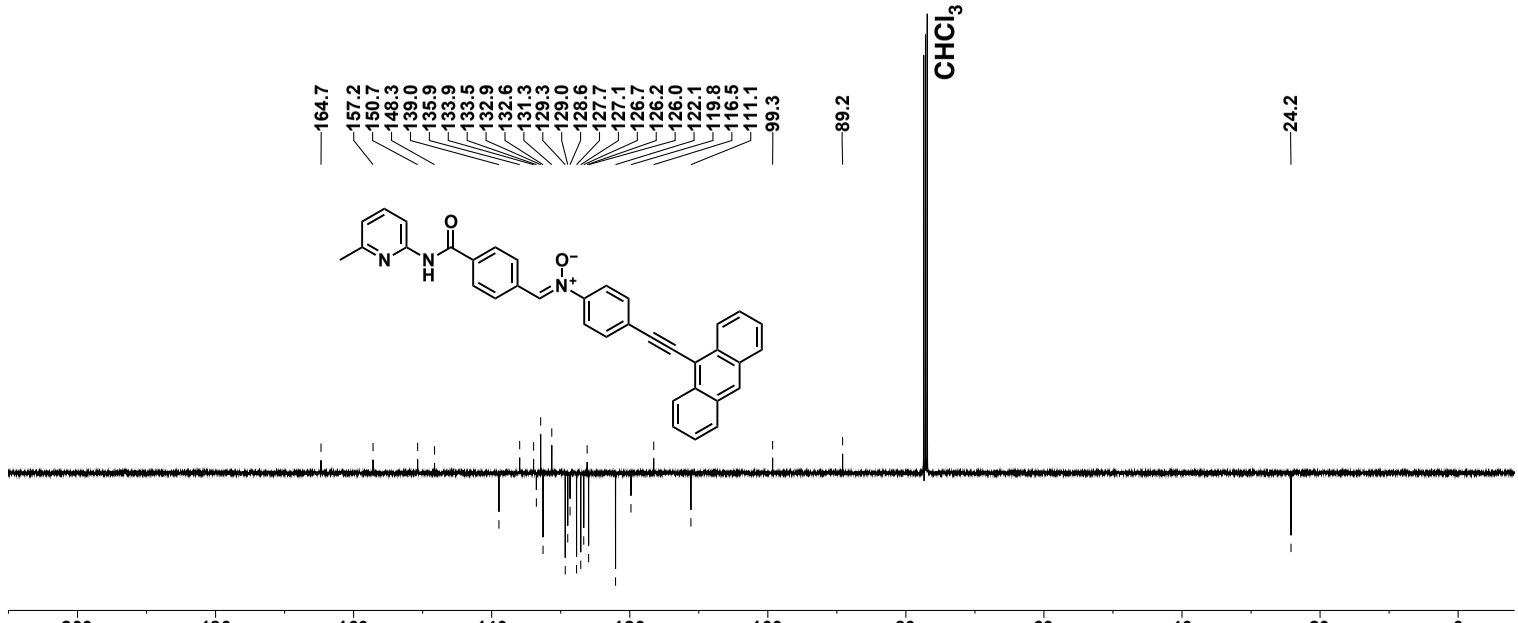


$^{13}$C NMR spectrum (125.8 MHz, RT, $CDCl_3$) of nitrone **1b**

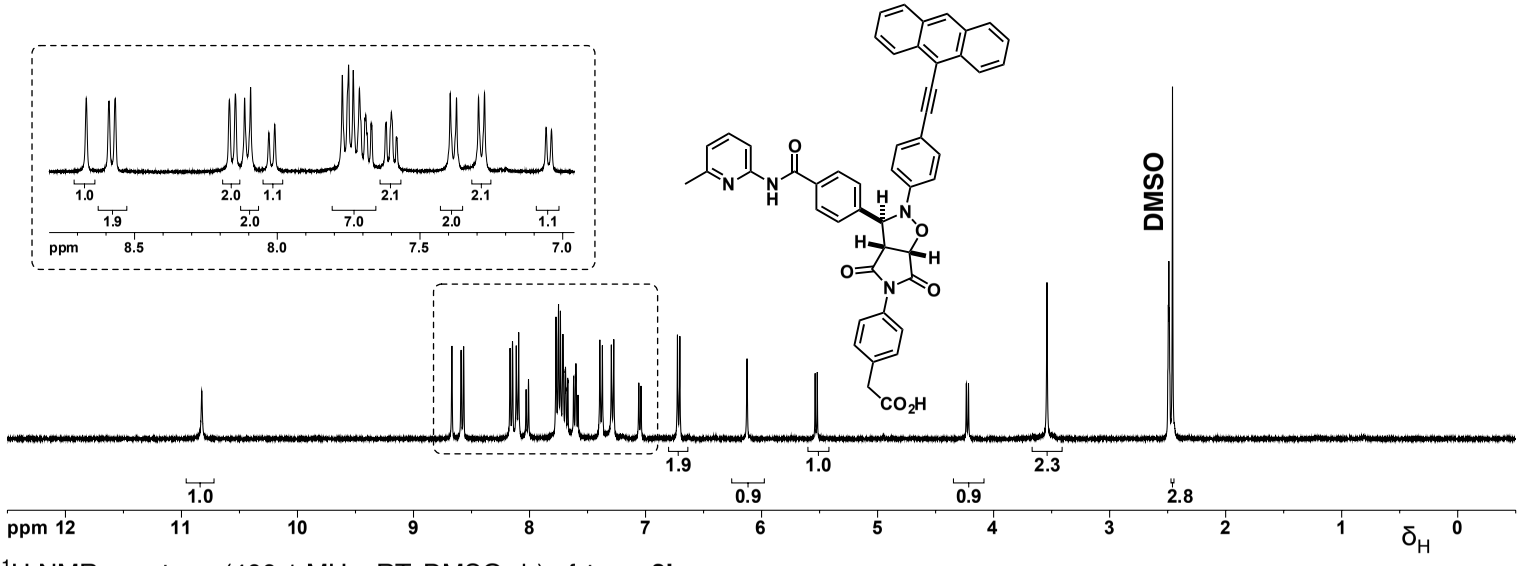


$^1$H NMR spectrum (400.1 MHz, RT, DMSO-$d_6$) of *trans*-**3b**

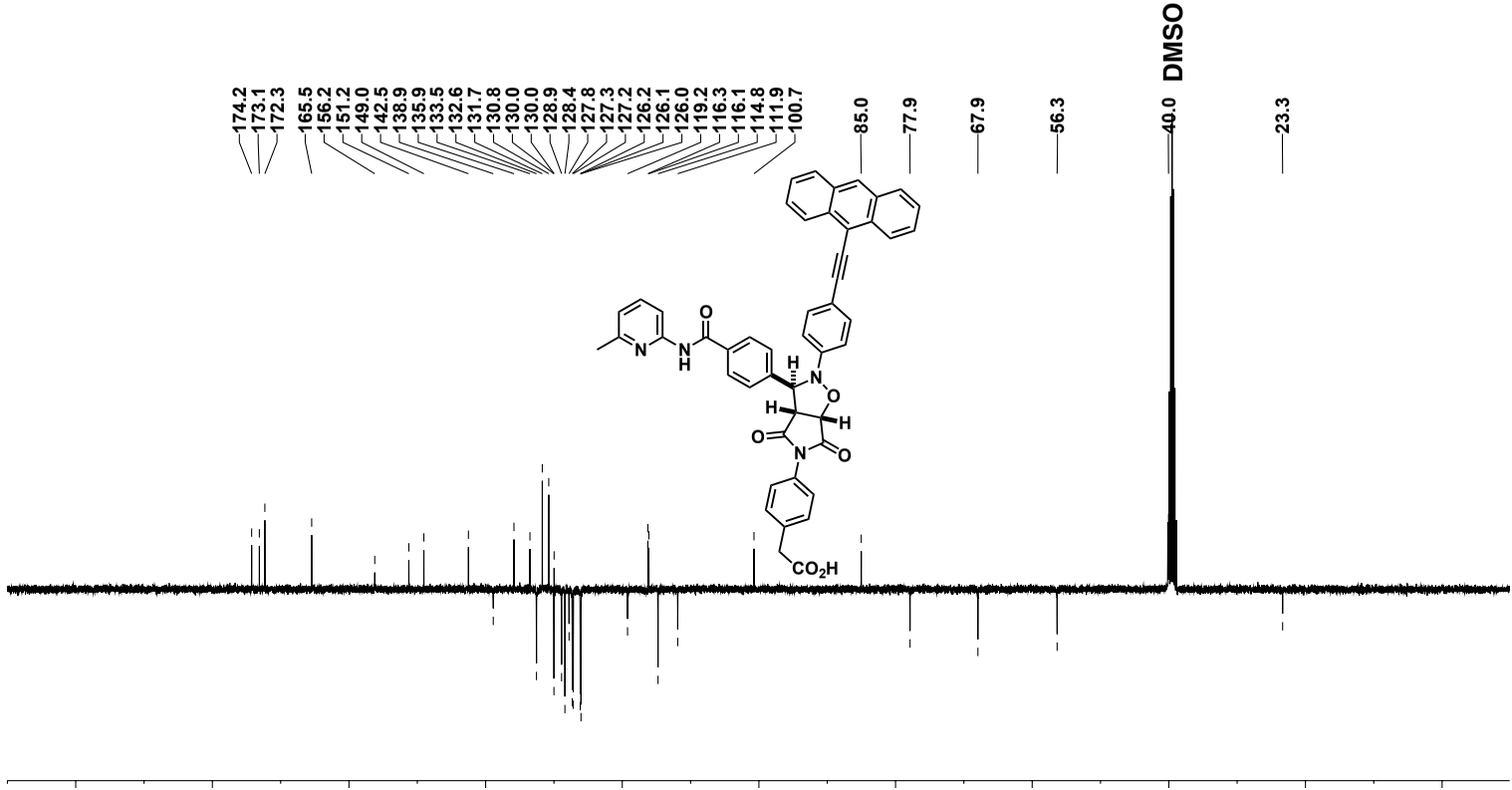


$^{13}$C NMR spectrum (100.6 MHz, RT, DMSO-$d_6$) of *trans*-**3b**

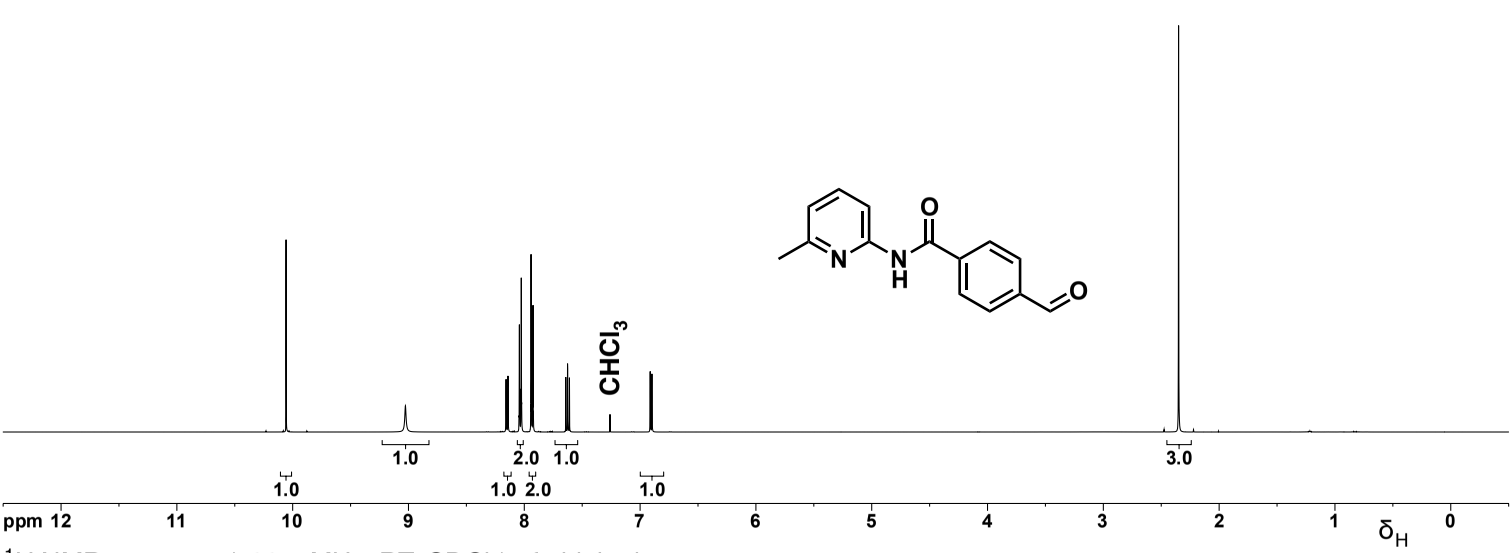


$^{1}$H NMR spectrum (500.1 MHz, RT, $CDCl_3$) of aldehyde

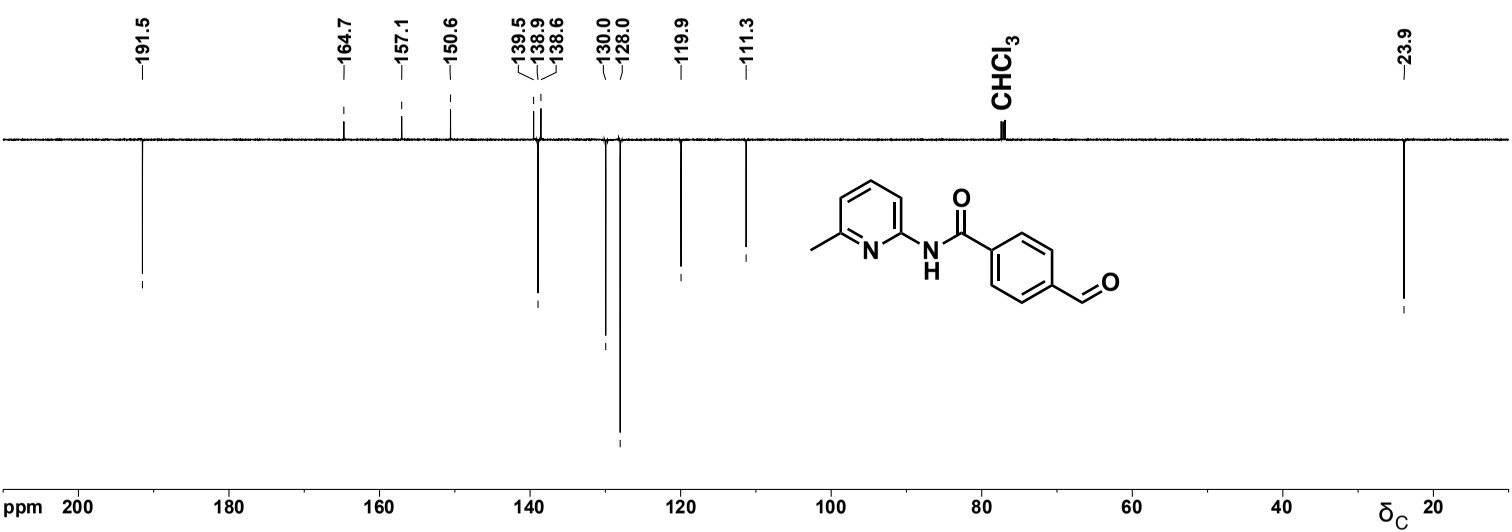


$^{13}$C NMR spectrum (125.8 MHz, RT, $CDCl_3$) of aldehyde

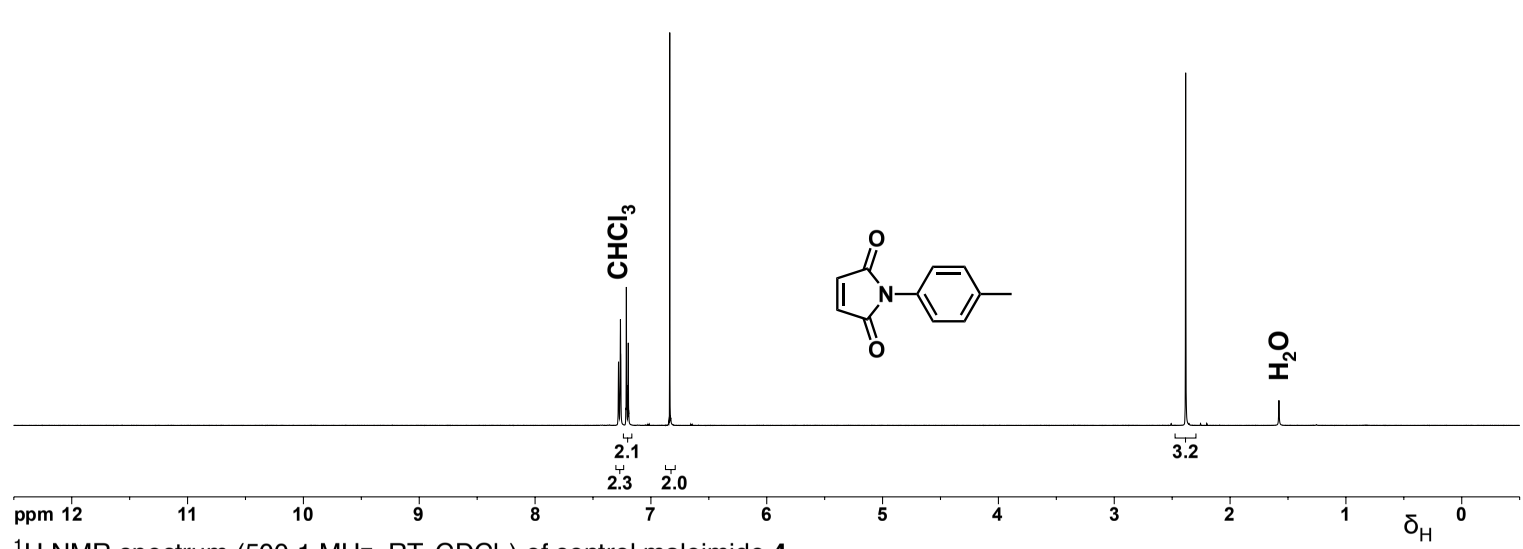


$^{1}$H NMR spectrum (500.1 MHz, RT, $CDCl_3$) of control maleimide **4**

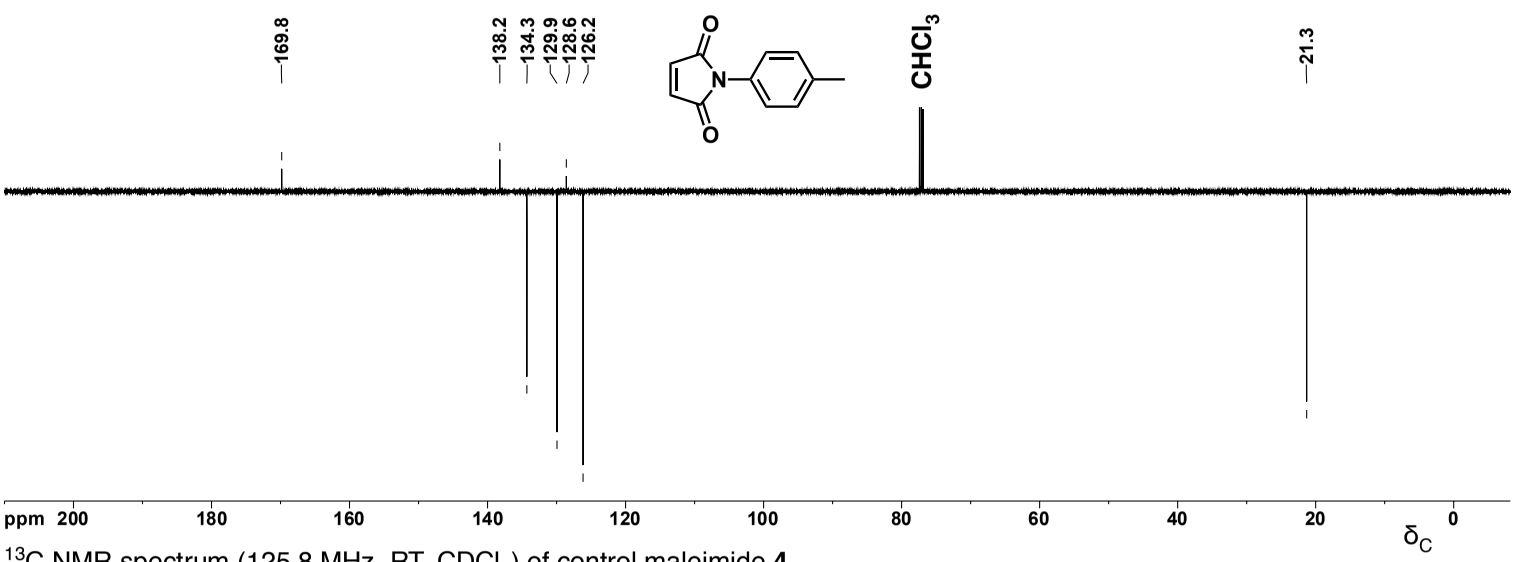


$^{13}$C NMR spectrum (125.8 MHz, RT, $CDCl_3$) of control maleimide **4**